Stephens et al., http://www.jcb.org/cgi/content/full/jcb.201208163/DC1

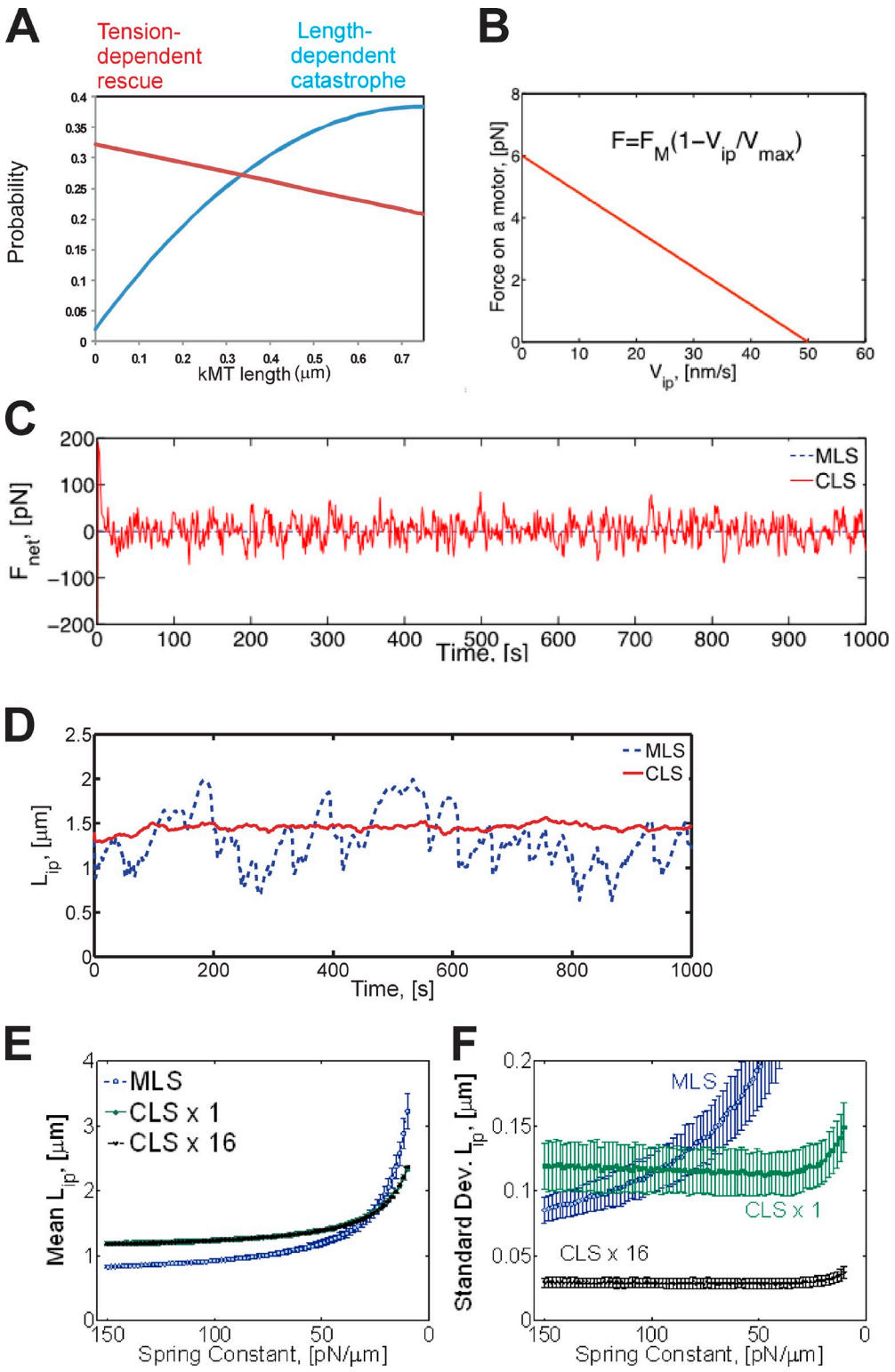

Figure S1. **Addition of experimentally measured kMT dynamics and motor on/off rates maintains trends of a minimal model.** (A) Fitted probabilities of switching kMT states based on tension-dependent rescue and length-dependent catastrophe (Gardner et al., 2005). (B) Motor velocity versus force on motor determined as a linear equation between maximum velocity (50 nm/s) and motor stall force (6 pN). (C) F_{net} in the MLS and CLS models. (D) Spindle length over time for MLS and CLS models. (E and F) Mean spindle length (E) and spindle variation (F) over a time lapse for MLS, CLS one spring, and CLS 16 springs upon decreasing the spring constant.

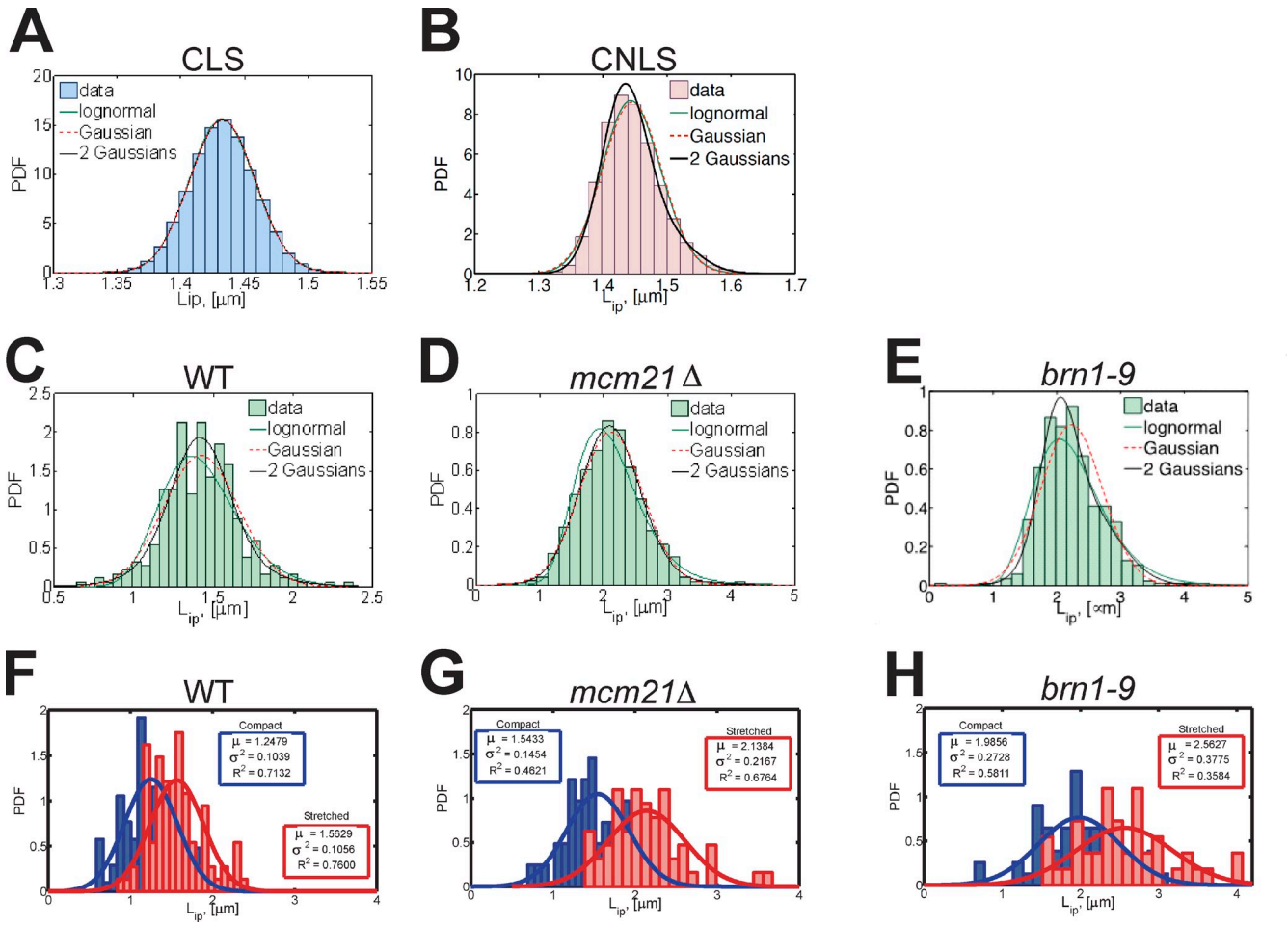

Figure S2. **Spindle length histograms of simulations and experimental conditions.** (A–E) Probability distribution functions of CLS WT (A) CNLS WT (B), experimental WT (C), experimental *mcm21Δ* depletion of pericentric cohesin (D), and experimental *brn1-9* depletion of condensin (E). Each histogram was fitted with a lognormal (green line), one Gaussian (red dotted line), and two Gaussian (black line). Lognormal and one Gaussian represent unimodal, whereas two Gaussian represents bimodal. R^2 values are given in Table S2. (F–H) Histograms of the spindle length distributions in WT (F), *mcm21Δ* (G), and *brn1-9* (H) cells with only compact LacO arrays versus cells with stretched LacO arrays. These graphs reveal two distinct populations in both WT and mutant cells (WT: $n = 218$, $P < 1.5 \times 10^{-11}$; *mcm21Δ*: $n = 106$, $P < 1.3 \times 10^{-10}$; *brn1-9*: $n = 106$, $P < 1 \times 10^{-6}$). Spindles with stretched LacO arrays are on average 500 nm longer and exhibit increased variance relative to spindles with compact LacO arrays. PDF, probability distribution function.

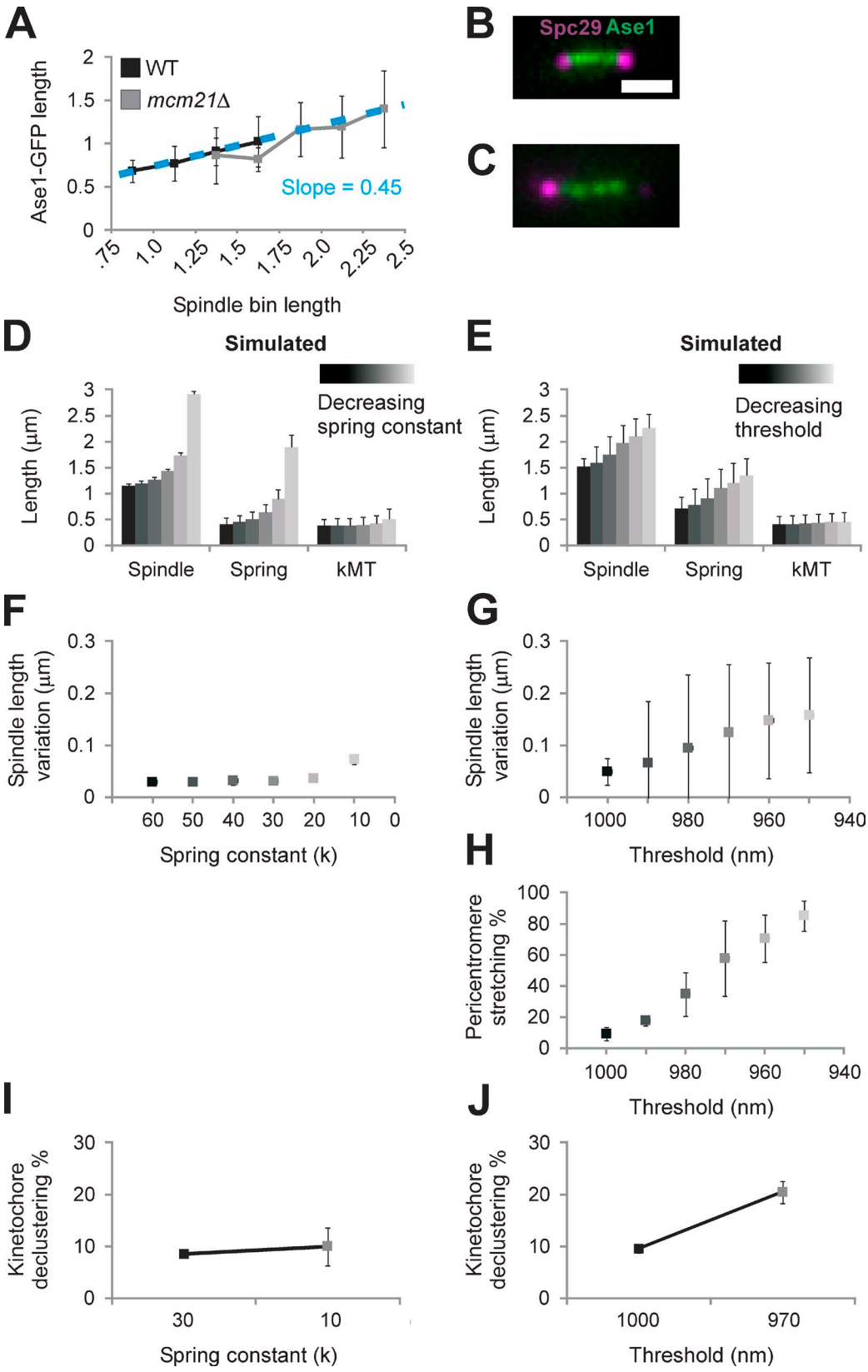

Figure S3. **The model is insensitive to overlap dynamics.** (A) Length of the Ase1-GFP signal for increasing spindle lengths in WT (n = 51) and *mcm21Δ* (n = 46) spindles. Ase1-GFP signal increases proportionally with spindle length with a slope of 0.45 (dotted blue line). (B and C) Example images of WT (B) and *mcm21Δ* (C) spindles labeled with Ase1-GFP and Spc29-RFP. (D–J) Simulations were run for the linear (CLS model, left column; D, F, and I) and piecewise (CNLS model, right column; E, G, H, and J) with increasing overlap zone dynamics from A. Spindle length (D and E), spindle variation (F and G), pericentromere stretching (H), and declustering (I and J) showed similar trends compared with the constant overlap zone (see Fig. 2, B and C, CLS and CNLS models, respectively). Error bars represent standard deviation. Bar, 1 μm.

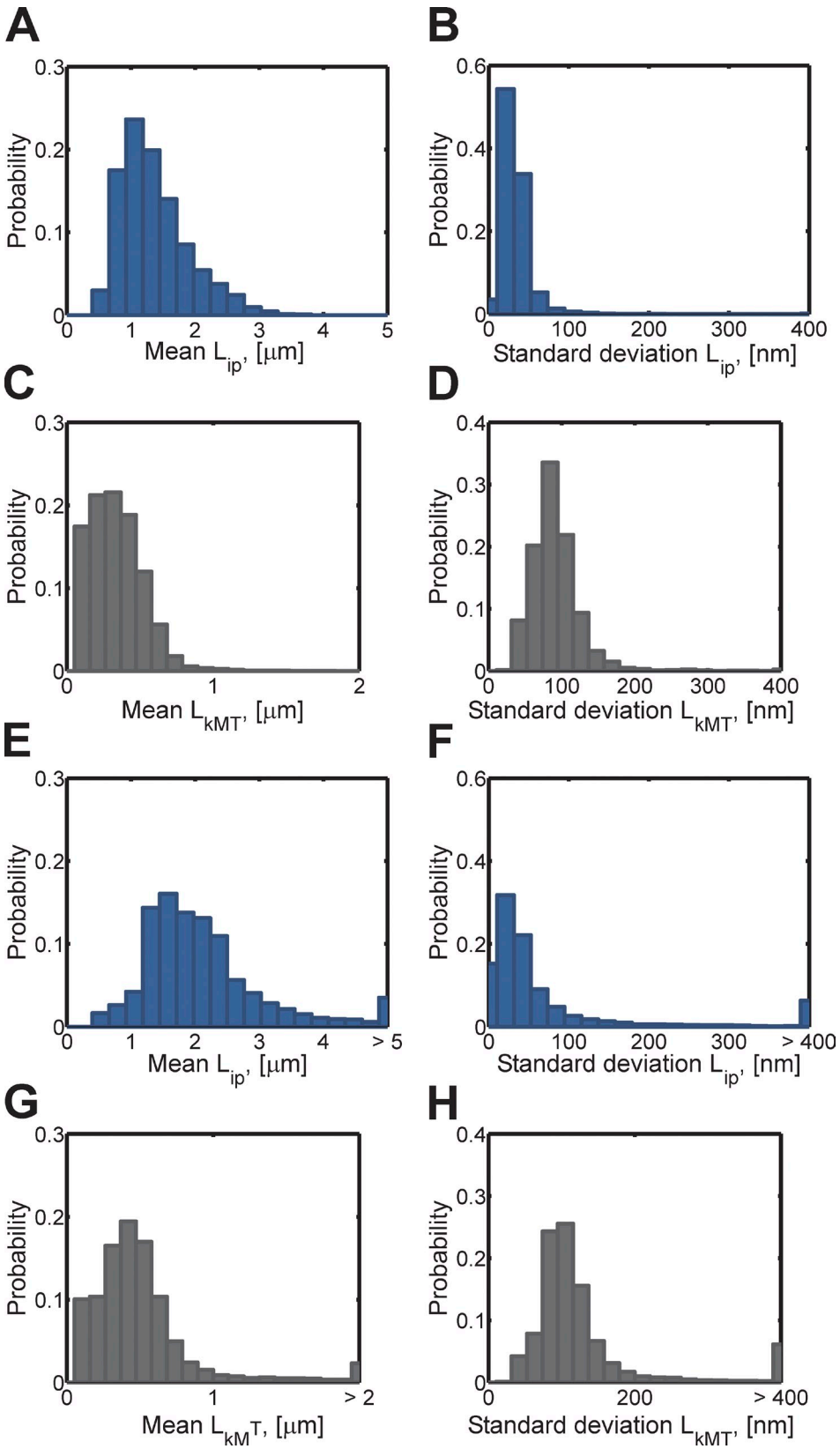

Figure S4. **Model sensitivity analysis reveals robustness of the model.** Values for the seven parameters are chosen randomly within each corresponding interval outlined in Table S3. (A–H) 10,000 random searches were performed using the CNLS with cross-links model with either a constant (A–D) and increasing (E–H) overlap region (L_{lap}). Histograms of spindle length (L_{ip}) mean (A and E) and standard deviation (B and F) and kMTs (L_{kMT}) length mean (C and G) and standard deviation (D and H) are shown. Clustering of spindle lengths in the histograms indicate that model predictions are tolerant to variations over wide intervals of parameter space. Spindle lengths >3 µm are considered as outliers. Sensitivity analysis of a model with a constant overlap zone generated outliers in <1% of simulations (74 out of 10,000), whereas a model with an overlap zone that increases proportionally with spindle length (Fig. S3) generated outliers in ∼14% of simulations (1,379 out of 10,000).

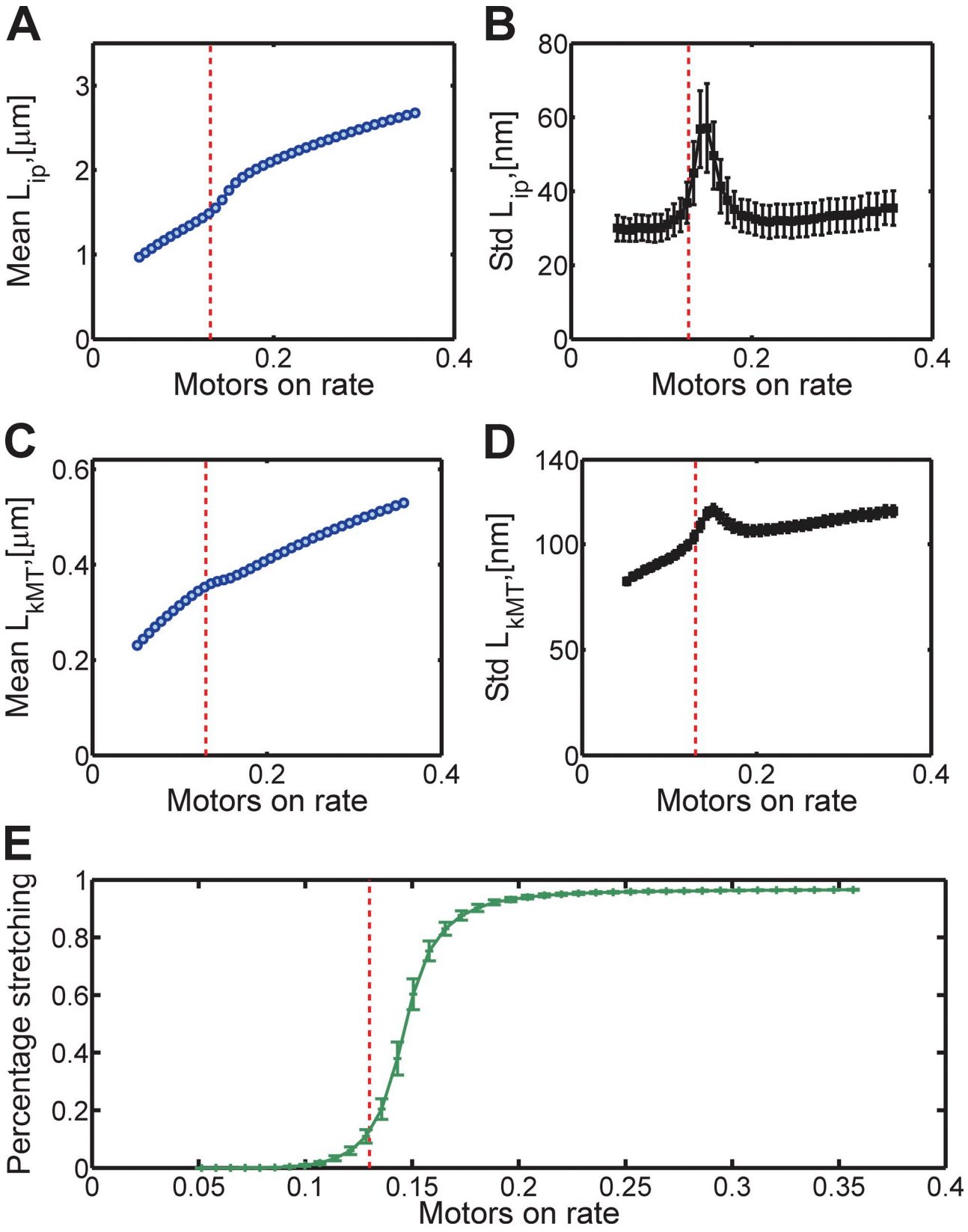

Figure S5. **The threshold for loop stretching disproportionally affects spindle length variation.** An example of single parameter analysis for the CNLS with cross-links model. (A–E) The effect of changing motor on rate on mean spindle length (A), standard deviation of spindle length (B), mean kMT length (C), standard deviation of kMT length (D), and loop stretching (E). Red lines denote WT default values. Spindle length varies monotonically with motor on rate. As expected, the addition of motors increases the extensional force, and therefore, spindle length increases. (B and D) In contrast, the standard (Std) deviation of spindle and kMT length is not monotonic. (E) A peak in standard deviation is coincident with threshold values in which 50% of the springs are stretched. This indicates that the threshold value is a sensitive parameter in the model.

Table S1. **Variable list**

Variable Name	Label	Description	Default values	Parameter source	In vivo values	Parameter relationships	Citations
Spindle length							
Spindle length	L_{ip}	Length of the spindle, from pole to pole	1.5×10^{-6} m	Measured; minimum 0.8×10^{-6} m because of overlap	WT: 1.5×10^{-6} m	L_{ip} is the integral of $V_{ip\ Lip\text{-}LkMT=Lspring}$	Winey et al., 1995; Stephens et al., 2011
Spindle velocity	V_{ip}	The speed at which the spindle grows/shrinks	–	Measured; observed range of -3.5–3.5×10^{-6} m/min	Shortening: $.54$–2.34×10^{-6} m/min; Growth: $.42$–1.6×10^{-6} m/min; No spring: 3.5×10^{-6} m/min	$V_{ip} = 3 \times 10^{-6}$ m/min $\times [1 + ((F_k + F_{drag})/F_{ip})]$	Motor speed: Hunt et al., 1994; Svoboda and Block, 1994. In vivo: Harrison et al., 2009; this paper
Outward motor force	F_{ip}	Outward force from the motors	2–3×10^{-10} N	–	–	$F_{ip} = D \times (6 \times 10^{-12}$ N)	Outward motor force
Inward spring force	F_k	Inward force from the springs	-2 to -3×10^{-10} N	–	–	$\Sigma F_k 1 \rightarrow F_k 16 = F_k$	
Drag force	F_{drag}	Drag force exerted on the spindle by viscosity	-5–5×10^{-12} N	–	–	$V_{ip} \times C_{drag} = F_{drag}$	
Drag coefficient	C_{drag}	Drag coefficient	3×10^{-5} Ns/m	Measured; model insensitive	175 poise $\times L_{ip}$	$V_{ip} \times C_{drag} = F_{drag}$ and $F_{ip} + F_k + F_{drag} = F_{net}$	Fisher et al., 2009
ipMTs and motors							
Overlap zone	L_{lap}	Length of the overlap zone	0.8×10^{-6} N/m	Measured; constant	–	L_{lap} is involved in single to double and free to single	Winey et al., 1995; Schuyler et al., 2003
Free motors	Free/U	Number of motors that are not bound to any microtubules	400	Total measured (bound and free); initial distribution insensitive	–	Involved in single to double and single to free	Unpublished data; J. Lawrimore, personal communication
Single-bound ipMT	Single ipMT	Number of motors singly bound to the ipMT	35 (×4 ipMT pairs, 140 total)	Initial distribution insensitive	–	Involved in single to free and free to single ipMt	Single-bound interpolar motors
Single-bound kinetochore motors	Single kMT	Number of motors singly bound to the kMTs	150	Initial distribution insensitive	–	Involved in single to free and free to single kMT	
Double-bound motors	D	Number of doubly bound motors in the overlap region (L_{lap})	10 (×4 ipMT pairs, 40 total)	Initial distribution insensitive	–	$Fip = D \times Nmotors$; D depends on functions double to single, free to single, single to double, and single to free	
Motor force	F_m	The force each individual motor exerts on the microtubule	6×10^{-12} N	Measured in vitro stall force	–	$F_{ip} = D \times F_m$	Hunt et al., 1994; Svoboda and Block, 1994
kMTs and Springs							
kMT length	L_{kMT}	Length of each kMT	350×10^{-9} m	Measured; 50×10^{-9} m minimum from EM	350×10^{-9} m, mean kMT	L_{kMT} switches stochastically between growth and shrinkage. Switching depends on F_k and L_{kMT}, respectively	Winey et al., 1995; Gardner et al., 2005
Growth rate	R_{gro}	Rate of growth for kMT	17×10^{-9} m/s	Measured (probability to switch states fitted)	17×10^{-9} m/s	The length added to each kMT is the integral of R_{gro}	Gardner et al., 2005
Shrinking rate	R_{shr}	Rate of shrinking for kMT	25×10^{-9} m/s	Measured (probability to switch states fitted)	25×10^{-9} m/s	The length subtracted from each kMT is the integral of R_{shr}	Gardner et al., 2005
Spring length	L_{spring}	Length of each chromatin spring	800×10^{-9} m	Measured aggregate interkinetochore distance	800×10^{-9} m	$L_{spring} = L_{ip} - (L^{left}{}_{kMT} + L^{right}{}_{kMT})$	Bouck and Bloom, 2007; Stephens et al., 2011

Table S1. **Variable list** *(Continued)*

Variable Name	Label	Description	Default values	Parameter source	In vivo values	Parameter relationships	Citations
Spring force	F_k^{ind}	Force of individual chromatin spring	–	–	–	If $L_{spring} < L_{threshold}$, $F_k^{ind} = k_1(L_{spring} - L_{rest1})$. If $L_{spring} \geq L_{threshold}$, $F_k^{ind} = k_2(L_{spring} - L_{rest2})$	
Looped spring constant	k_1	Spring constant of looped chromatin	30×10^{-6} N/m	Free; explored $5-150 \times 10^{-6}$ N/m	–	If $L_{spring} < L_{threshold}$ $F_k^{ind} = k_1(L_{spring} - L_{rest1})$	
Unlooped spring constant	k_2	Spring constant of unlooped chromatin	–	–	–	$k_2 = k_1 \times [L_1/(L_1 + L_{openloop})]$. If $L_{spring} \geq L_{threshold}$, $F_k^{ind} = k_2(L_{spring} - L_{rest2})$	
Looped rest length	L_{rest1}	Rest length of looped under no force	200×10^{-9} m	Estimated from measured	$<250 \times 10^{-9}$ m	If $L_{spring} < L_{threshold}$, $F_k^{ind} = k_1(L_{spring} - L_{rest1})$	Bystricky et al., 2004
Unlooped rest length	L_{rest2}	Rest length of unlooped under no force	650×10^{-9} m	–	$>250 \times 10^{-9}$ m	$L_{rest2} = L_{rest1} + L_{openloop}$	
Threshold	$L_{threshold}$	The spindle length at which the loop comes undone	975×10^{-9} m (best-fit WT)	Free; explored $1.1–0.8 \times 10^{-6}$ m	–	Deterministic length at which spring switches from k_1 to k_2 and L_{rest1} to L_{rest2}	
Loop length	$L_{openloop}$	The length of the loop	450×10^{-9} m	Estimated from measured[a]	10-kb LacO = 450×10^{-9} m of 11-nm fiber	Used to calculate k_2 and L_{rest2}	Stephens et al., 2011
Loop stretching		The loop in the spring has come undone	–	True or false	10% of the time in WT	If stretched is true, the spring is not looped. If stretched is false, the spring is looped.	
Cross-linking spring constant	$k_{cross\text{-}link}$	Spring constant of cross-links	9×10^{-6} N/m (best-fit WT)	Free; explored $0–15 \times 10^{-6}$ N/m	–	$F_k^{cross\text{-}link} = F_k - k_{cross\text{-}link}(L_{spring}^{n-1} - L_{spring}^{n+1})$	This paper

[a]WT mean axial distance between a 1.7-kb LacO and a 6.8-kb LacO focus translates into a 102-bp/nm compaction. The mean axial distance between a WT 1.7-kb LacO to a stretched 6.8-kb LacO has an increase in distance (50–189 nm), which translates into a 27-bp/nm compaction and is consistent with extended nucleosomal compacted chromatin (11-nm fiber).
Minus signs indicate not available.

Table S2. **Statistics of the Gaussian distributions shown in Fig. S2**

R^2 fit	WT	*mcm21D*	*brn1-9*	CLS	CNLS
One Gaussian	0.8895	0.9732	0.9364	0.9971	0.9788
Lognormal	0.8699	0.9502	0.9457	**0.998**	0.9813
Two Gaussians	**0.8977**	**0.9792**	**0.9742**	**0.998**	**0.9971**
n	317	756	496	9,000	9,000

Bold numbers denote best fit.

Table S3. **Sensitivity analysis parameters and range**

Parameter	Default	Min	Max	Equation
MT rescue rate (1/s)	0.017	0.01	0.03	
MT catastrophe rate (1/s)	0.025	0.015	0.035	
Single to double on rate (1/s)	0.13	0.005	0.16	
Double to single off rate (1/s)	0.3	0.2	0.4	
Overlap length constant C_0 (µm)	0.8	0.5	1	$L_{lap} = C_0$
	0.5	0.3	0.7	$\Delta L_{lap} = C_0 \Delta L_{ip}$
Rescue probability C_1	1	0.2	1.8	$p_r = 0.21 - C_1 \times 9.5F_k$
Catastrophe probability C_1				$p_c = 0.27 + C_1 \times 0.442\ (L_{kMT} - 0.34)$

MT, microtubule.

Table S4. **MLS model parameters**

Parameter	Notation	Default value
Spring constant	k_{sp}	22 pN/µm
Drag coefficient	C_{drag}	30 pN/s/µm
Motor detachment rate	k_{off}	0.25 motors/s
Motor attachment rate	k_{on}	0.5 motors/s
Mean of L_{kMT}	L_m	0.4 µm
Standard deviation of L_{kMT}	σ_m	0.088 µm
Spring rest length	l_r	0.2 µm

Table S5. **Motor on/off rates**

Rate	Description	Dependence	Value	Notes
$k_{on,1}$	Attachment rate of single-bound motors to ipMTs	Constant	0.13 s^{-1}	a
$k_{on,2}$	Attachment rate of unbound motors to ipMTs	$L_{ip}, L_{kMT}^{left,right}$		b
$k_{on,3}$	Attachment rate of unbound motors to kMTs	$L_{ip}, L_{kMT}^{left,right}$		b
$k_{off,1}$	Detachment rate of double-bound motors	Constant	0.3 s^{-1}	c
$k_{off,2}$	Detachment rate of single-bound motors	Constant	0.3 s^{-1}	c

a, b, and c refer to corresponding labels in Materials and methods subsection Motor dynamics.

References

Bouck, D.C., and K. Bloom. 2007. Pericentric chromatin is an elastic component of the mitotic spindle. *Curr. Biol.* 17:741–748. http://dx.doi.org/10.1016/j.cub.2007.03.033

Bystricky, K., P. Heun, L. Gehlen, J. Langowski, and S.M. Gasser. 2004. Long-range compaction and flexibility of interphase chromatin in budding yeast analyzed by high-resolution imaging techniques. *Proc. Natl. Acad. Sci. USA*. 101:16495–16500. http://dx.doi.org/10.1073/pnas.0402766101

Fisher, J.K., M. Ballenger, E.T. O'Brien, J. Haase, R. Superfine, and K. Bloom. 2009. DNA relaxation dynamics as a probe for the intracellular environment. *Proc. Natl. Acad. Sci. USA*. 106:9250–9255. http://dx.doi.org/10.1073/pnas.0812723106

Gardner, M.K., C.G. Pearson, B.L. Sprague, T.R. Zarzar, K. Bloom, E.D. Salmon, and D.J. Odde. 2005. Tension-dependent regulation of microtubule dynamics at kinetochores can explain metaphase congression in yeast. *Mol. Biol. Cell*. 16:3764–3775. http://dx.doi.org/10.1091/mbc.E05-04-0275

Harrison, B.D., M.L. Hoang, and K. Bloom. 2009. Persistent mechanical linkage between sister chromatids throughout anaphase. *Chromosoma*. 118:633–645. http://dx.doi.org/10.1007/s00412-009-0224-6

Hunt, A.J., F. Gittes, and J. Howard. 1994. The force exerted by a single kinesin molecule against a viscous load. *Biophys. J.* 67:766–781. http://dx.doi.org/10.1016/S0006-3495(94)80537-5

Schuyler, S.C., J.Y. Liu, and D. Pellman. 2003. The molecular function of Ase1p: evidence for a MAP-dependent midzone-specific spindle matrix. *J. Cell Biol.* 160:517–528. http://dx.doi.org/10.1083/jcb.200210021

Stephens, A.D., J. Haase, L. Vicci, R.M. Taylor II, and K. Bloom. 2011. Cohesin, condensin, and the intramolecular centromere loop together generate the mitotic chromatin spring. *J. Cell Biol.* 193:1167–1180. http://dx.doi.org/10.1083/jcb.201103138

Svoboda, K., and S.M. Block. 1994. Force and velocity measured for single kinesin molecules. *Cell*. 77:773–784. http://dx.doi.org/10.1016/0092-8674(94)90060-4

Winey, M., C.L. Mamay, E.T. O'Toole, D.N. Mastronarde, T.H. Giddings Jr., K.L. McDonald, and J.R. McIntosh. 1995. Three-dimensional ultrastructural analysis of the *Saccharomyces cerevisiae* mitotic spindle. *J. Cell Biol.* 129:1601–1615. http://dx.doi.org/10.1083/jcb.129.6.1601

A PDF file is provided that shows the mitotic spindle simulation manual.

A ZIP file is provided containing the mathematical model.